KSCE Journal of Civil Engineering (2015) 19(5):1385-1395
Copyright ⓒ2015 Korean Society of Civil Engineers
DOI 10.1007/s12205-014-0626-8

Structural Engineering

pISSN 1226-7988, eISSN 1976-3808
www.springer.com/12205

Impact Strength of Hybrid Steel Mesh-and-Fiber Reinforced Cementitious Composites

P. B. Sakthivel*, A. Ravichandran, and N. Alagamurthi*****

Received October 17, 2013/Revised June 12, 2014/Accepted July 19, 2014/Published Online December 31, 2014

Abstract

Large volumes of concrete are produced for construction purposes which creates sustainability issues. Therefore, some of the alternatives to concrete that are being researched and implemented are Steel Mesh Reinforced Cementitious Composites (SMRCC) and Fiber Reinforced Cementitious Composites (FRCC). But due to limitations in element thickness and volume percentage of reinforcement in SMRCC and FRCC, this study has made an attempt to develop Hybrid Steel Mesh-and-Fiber Reinforced Cementitious Composites (HSMFRCC) and study its impact performance. Thus, in order to evaluate the energy absorption of HSMFRCC, 250 mm × 250 mm × 25 mm (thick) slab elements were cast with various combinations of 3-5 layers of steel weld mesh and SS fibers of 0.5-2.5% (of volume of specimens) and low velocity repeated drop weight impact test was administered. From the experimental results, it was found that the impact resistance of HSMFRCC (test specimens) is higher than SMRCC (control specimens using only steel mesh as reinforcement). Regression models have been developed in this study and validated using new hybrid mesh and fiber reinforcement mix. The predicted regression equations developed for initial and ultimate impact energy absorption of cementitious composites with hybrid steel mesh and fibers will be quite useful to the practitioners.

Keywords: *energy absorption, fibers, mechanical properties, mesh, regression, statistical models*

1. Introduction

Sustainability in building construction has significant relationship with the ultimate survival of humanity. In developing countries, there is a wide expansion of urban spaces and extension of city limits to manage urbanization, as a result of which, large number of modern buildings in aesthetically appealing forms are constructed. Concrete is presently the most widely used construction material and the same trend is expected in the foreseeable future. But the disadvantage of concrete is that it consumes large amount of raw materials resulting in depletion of global natural resources and environmental degradation. For example, natural gravel stones used in concrete is sourced from quarrying operations, and the related activities viz., drilling, cutting, removal and lifting of big-size boulders, crushing or sizing-down and separation activities needs fossil fuels for all its machinery works and transportation activities causing sustainability concerns (Sakthivel *et al*., 2014a; 2014b). Similarly, large quantities of sand which is mined from river beds for use as fine aggregates in concrete not only affects the fresh drinking water sources but also the flora and fauna creating an imbalance in the eco system.

The concrete's key binding agent, cement, consumes natural fuel energy sources during the manufacturing processes, i.e., for production of one tonne of Ordinary Portland Cement (OPC), 60-130 kg of fuel oil or equivalent (depending upon the cement variety and the process used) and about 110 KWh of electricity are consumed which releases gaseous CO_2 during calcination (Sakulich *et al*., 2011; Shaikh, 2013; Cachim *et al*., 2014). Thus, the production and use of Portland Cement has high environmental impacts from greenhouse gas emissions and overall energy usage. It has been estimated that Portland Cement Concrete is responsible for approximately 7% of worldwide greenhouse gas emissions from the calcination process of raw materials with over 1 tonne of carbon dioxide (CO_2) emitted for each tonne of Portland cement produced (Tassew and Lubell, 2014).

Sustainability can be achieved by keeping stock of the scarce natural resources for future generation and restoring the ecosystems (Sakthivel and Jagannathan, 2012a, 2012b). Therefore, it is hightime that new sustainable composite materials are innovated that utilizes minimum quantities of natural resources but ultimately gives high strength, toughness, energy absorption and durability (Kuder *et al*., 2006; Farnam *et al*., 2010; Pereira *et al*., 2012; 2013; Shaikh, 2013; Zhou *et al*., 2013; Xin *et al*., 2014).

Few alternative materials to conventional concrete that have

*Ph.D. Research Scholar, Dept. of Civil Engineering, Pondicherry Engineering College, Puducherry-605014, India (Corresponding Author, E-mail: pbs_ms@yahoo.com)
**Professor, Dept. of Civil Engineering, Christ College of Engineering & Technology, Puducherry-605010, India (E-mail: principal@christcet.edu)
***Professor, Dept. of Mechanical Engineering, Pondicherry Engineering College, Puducherry-605014, India (E-mail: alagu_pec@yahoo.co.in)

been widely researched and practically implemented in several construction projects worldwide in the last few decades (with element thickness of 10-25 mm) are Steel Mesh Reinforced Cementitious Composites (SMRCC) (traditionally known as ferrocement) and Fiber Reinforced Cementitious Composites (FRCC). While the former uses steel mesh, the latter uses metallic or non-metallic fibers as reinforcement in hydraulic cement mortar (sand, cement and water with total elimination of coarse aggregates) (Sakthivel and Jagannathan, 2012a; 2012b; Sakthivel *et al*., 2012). In SMRCC, there are constraints in increasing the number of mesh layers due to limitation of 10-25 mm thickness, as high volume fraction of steel mesh in mortar mix may spall or extreme tensile layer delaminate and fail (Shannag and Ziyyad, 2007). Similarly, in FRCC which uses randomly oriented discontinuous fibers into a cementitious matrix (Suthiwarapirak *et al*., 2004; Sakthivel *et al*., 2012), the volume percentage of fibers (metallic or non-metallic discontinuous type) is limited to 2.5% beyond which difficulty in mixing or casting of the fibrous mortar is experienced (Sakthivel *et al*., 2014b, 2014c).

Many types of discontinuous fibers (made of steel, glass, carbon and polymer based) with variable strength and dimensions are available in the market (Cavdar, 2014) which brings new opportunities for cement-based composites to improve the toughness and energy absorption capacity (Pereira *et al*., 2012; Shaikh, 2013) and ductility (Almusallam *et al*., 2013) but the selection of appropriate fiber type is crucial (Tosun-Felekoglu and Felekoglu, 2013). Steel fiber is popularly used as is associated with the fact that steel presents a good affinity with cementitious composites (Sakthivel *et al*., 2014b), the ease of use, the high toughness and resistance to static and dynamic loads (Holschemacher *et al*., 2010; Rambo *et al*., 2014). The steel fiber is said to have the ability to create a mechanical bond with cement-matrix (Peled and Shah, 2003) and reduce the damage that a cement-based material may suffer during an impact (Soe *et al*., 2013). One of the methods to evaluate the toughness and energy absorption of the material is by conducting impact tests. In practical situations, the unexpected structural falling loads (of low velocity of 30 m/sec) or accidental drop weights on structural elements should be considered, for example, the falling debris on concrete slab during the demolition works in the neighboring areas may result in catastrophic failure of the structural element endangering the lives of the people. To minimize the damage and prevent collapse, these structures must possess a much greater resistance to impact (Elavenil and Knight, 2012). Impact resistance is related to the capacity to provide safety in use and to guarantee its performance after impact (Shaheen *et al.*, 2013). Therefore, in order to enhance public safety (Yang and Li, 2012; Ren *et al*., 2013), the researchers and engineers should develop stronger and tougher cementitious composites (Maalej *et al*., 2005) with ductile characteristics (Almusallam *et al.*, 2013) that are capable of absorbing high level of impact energy and without getting easily damaged or collapsed (Yang and Li, 2012; Aldousiri *et al*., 2013; Ren *et al*., 2013).

Impact loading of structural members involves complex process where both structural and material parameters can influence their performance (Ong *et al*., 1999). In order to evaluate the impact energy absorption of composite materials, various scientific methods are employed such as dropping weight single or repeated impact test, weighted pendulum type impact test, projectile impact test, explosion-impact test, constant strain rate test, split-hopkinson bar test and instrumented pendulum impact test (Elavenil and Knight, 2012; Aldousiri *et al*., 2013; Zhou *et al*., 2013). But out of these various tests, the impact resistance assessed by Low-Velocity Impact (LVI) tests using repeated drop weight is widely recommended by researchers and practitioners as the procedure is simple to administer, and the number of blows that cause the distress in the specimen can be easily determined (ACI 544; Sakthivel and Jagannathan, 2012a, b; Sakthivel *et al.*, 2012, 2014c). In LVI tests, the composite material is struck by an impact force or projectile of known mass from a fixed height or determined velocity, and on repeated loading, the material undergoes changes and develops cracks depending upon its energy absorbing capacity, and dissipates energy in the elements and ultimately deforms from its original shape and fails (Sakthivel *et al*., 2014c).

Farnam *et al.* (2010) have used drop weight impact testing apparatus with 8.5 kg steel cylindrical projectile with 50 mm diameter and 550 mm height. The projectile was dropped on the High Performance Fiber Reinforced Cementitious Composite Panel of size 300 mm × 300 mm × 23 mm (thickness) from one meter height periodically until the failure occurred. The failure pattern, crack propagation and crack width in various sides of specimens were measured and recorded during the experiments at the end of each impact. In another study, Shaheen *et al.* (2013) have used low velocity impact test to determine the energy absorption of SMRCC (ferrocement) plates of size 500 mm × 500 mm × 25 mm (thickness); and the falling load was kept at 1.15 kg at a height of 1.12 m. The increase in the number of weld mesh layers from 3 to 4 and 4 to 5 has shown a corresponding increase in the energy absorption of plate elements. Use of polypropylene synthetic fibers resulted in retarding the occurrence of the first crack and better crack distribution in the elements. Similarly, Al-Hadithi and Al-Nu'man (2008) conducted low-velocity impact tests on polymer-modified concrete of square slabs of 500 mm × 500 mm × 50 mm (thickness) of repeated falling mass of 1300 gm steel ball freeling falling from three heights 2400 mm, 1200 mm and 830 mm, and the maximum increase in LVI resistance are 33.33%, 75% and 83.33% at ultimate failure, and it was found that the impact resistance represented by number of blows until failure decreases with the increase in falling mass height.

In the study of Kaleemulla and Siddeswarappa (2011), LVI drop weight method was employed with low velocity impact range not exceeding 30 m/sec. A repeated drop weight impactor (2.5 kg and 4.8 kg) with steel hemispherical end of 20 mm diameter bolted to a steel cylinder were used to give a central impact on the centre of plates with an impact velocity of 3.13 m/

s using impactor height of 0.5 m, allowing the hammer to slide freely along a guide in the vertical direction. The delamination area and indentation depth were measured as a fraction of the drop number; and the results showed that the impactor with 12.26 J required more number of impacts to fail the composite in comparison to impactor with 23.54 J.

Tabatabaei *et al.* (2014) have studied the comparative impact behaviour of Long Carbon Fiber Reinforced Concretes (LCFRC) by falling weight impact tests using impact testing apparatus. They dropped a steel rod (70 mm diameter, and 23 kg weight) from a prescribed height on to the mid-span of a panel (placed in simply supported condition on all 4 sides), recorded the drop weight by visually observing the first crack and determined the ultimate failure based on the drop weight required to sufficiently open the crack and fracture the panel. After first crack, the energy for failure has increased for LCFRC panels in comparison to the reference specimens (without fibers) due to the interlocking mechanism of fibers with the matrix; and LCFRC panels have shown higher impact resistance than the reference panels.

Sakthivel *et al.* (2014c) have conducted LVI tests on cementitious composite slab elements with hybrid reinforcement mix of steel mesh (3 to 5 layers) and polyolefin fibers (0.5 to 2.5%) by repeatedly dropping steel ball of weight 29.43 N from a height of 600 mm. The specimens were able to sustain large amount of impact (after first crack) before it ultimately failed demonstrating high level of energy absorption in the slab elements (Mo *et al*., 2014). Thus, the study of Sakthivel *et al.* (2014c) have remarkably shown that hybrid mesh and fiber reinforced composites are toughened high performance materials capable of withstanding the impact loads; and a synergy is created in the hybridization process (Yun *et al*., 2007; Kim *et al*., 2008; Colombo *et al*., 2010; Trainor *et al*., 2013; Tosun-Felekoglu and Felekoglu, 2013) of combining two types of reinforcements, mesh and fibers.

Narendar *et al.* (2014) have motivated that hybrid reinforced composites imply a step beyond in the search for novel materials with improved mechanical properties and/or reduced cost. While selecting new composites with hybrid reinforcement, the response to impact and total energy absorbed by the element must be assessed (Kaleemulla and Siddeswarappa, 2011). While Sakthivel and Jagannathan (2012a; 2012b) have conducted LVI tests on SMRCC and Sakthivel *et al.* (2012) on FRCC reinforced with Stainless Steel (SS) fibers, the present study is to combine steel mesh and SS fiber reinforcement in hybrid form and determine the impact performance of Hybrid Steel Mesh-and-Fiber Reinforced Cementitious Composites (HSMFRCC) (test specimens) and also compare these results with that of SMRCC (control specimens). Also, it is proposed by the present authors to develop statistical modeling equations from experimental results (Sayed-Ahmed, 2012; Sahmaran *et al*., 2013; Sakthivel *et al.*, 2014a; 2014b; 2014c) to predict the Initial Impact Energy Absorption (IIEA) and Ultimate Impact Energy Absorption (UIEA) of HSMFRCC.

2. Experimental Work

2.1 Materials

Ordinary Portland Cement (OPC-53 Grade) conforming to IS 12269-1987 (2008) with specific gravity of 3.37 and locally available natural river sand conforming to Zone II of IS 383: 1987 (2007) with fineness modulus of 2.92 and specific gravity of 2.61 were used (Ramasamy, 2012) in this study. Well-graded sand passing through 2.36 mm sieve was used to prepare the cement mortar (ACI 549R, 1997; Lin *et al*., 2011; Ibrahim, 2011; Mohammed and Assi, 2011; Sakthivel and Jagannathan, 2012a; 2012b; Sakthivel *et al*., 2012; 2014a; 2014b; 2014c). Potable water was used for mixing the cement mortar and curing the specimens.

The galvanized steel weld mesh (with diameter of 0.70 mm and grid spacing of 12.5 mm × 12.5 mm) which is locally available has been used. The tensile strength and yield stress of the mesh are 512.36 N/mm^2 and 406.51 N/mm^2 respectively, and elongation 7.12%. The non-corrosive Stainless Steel (SS) fibers (crimped type) of 12.5 mm length manufactured by Stewols India (P) Ltd. are used in this study. The ultimate tensile strength of the fibers is 1353.00 N/mm^2

2.2 Methods

2.2.1 Mortar Strength

The cement mortar is prepared using sand-cement (s/c) ratio of 2:1 and water-cement (w/c) ratio of 0.43 by weight, which was fixed after several trials by the present authors and finalized

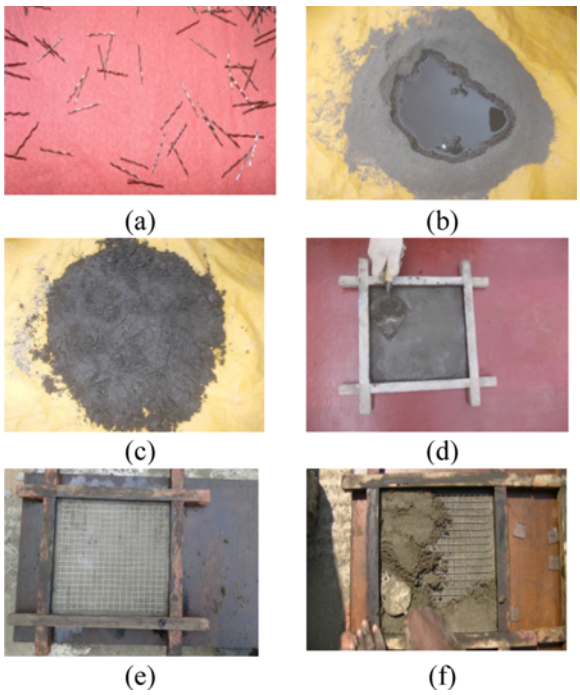

Fig. 1. Casting of Specimens: (a) Stainless Steel Fibers (Crimped Shape), (b) Water Added to Fibrous Cement Mortar, (c) SS-Fibrous Wet Cement Mortar, (d) Slab Casting with Mortar using Hand Pressure and Even Finishing of the Layer, (e) Mesh Placed over the Mortar, (f) Mortar over Mesh

based on the average values used in the previous studies (Naaman, 2000; Shannag, 2008; Ibrahim, 2011; Sakthivel and Jagannathan, 2012a; 2012b; Sakthivel *et al*., 2012; 2014a; 2014b; 2014c).

For control specimens, water is directly added to the dry cement mortar and mixed well. For test specimens, the required amount of crimped SS fibers (varying fiber percentage of 0.5%, 1%, 1.5%, 2% and 2.5% of volume of specimens) as shown in image 1a-Fig. 1 is evenly spread to the dry cement and then mixed; and then the water (as per the above w/c ratio) is added to dry SS fibrous mortar as shown in image 1b-Fig. 1 and thoroughly mixed. No workability problems were experienced during mixing of the fibrous mortar with SS fibers 0.5-2.5% and a homogenous mixture as shown in image 1c-Fig. 1 was obtained.

The cylinder compressive and splitting-tensile test were determined using cylindrical moulds of size of 100 × 200 mm (height) (Shaheen *et al*., 2013; Sonebi and Bassuoni, 2013). The cylinder Compressive Strength (CS) (at 28 days) of SS-fibrous cement mortar was found to be 30.14, 31.00, 33.54, 36.52 and 38.22 N/mm^2 (using SS fibers of 0.5%, 1%, 1.5%, 2% and 2.5% respectively) in cementitious matrix, when compared to CS at 28 days of control specimens (cast with plain cementitious matrix without fibers) of 25.48 N/mm^2.

The Split-Tensile Strength (TS) (at 28 days) have shown 5.63, 6.79, 7.21, 7.64 and 8.28 N/mm^2 for SS fibrous cement mortar using SS fibers of 0.5%, 1%, 1.5%, 2% and 2.5% respectively, when compared to TS of control specimens (at 28 days) (using plain cement mortar without SS fibers) of 4.56 N/mm^2.

The Flexural Strength (FS) (at 28 days) of SS fibrous cement mortar using prismatic beam moulds of size 40 mm × 40 mm × 160 mm (Ibrahim, 2011; Molero *et al*., 2011; Cheah and Ramli, 2012; Yardim *et al*., 2013; Yu *et al*., 2014) have shown 5.94, 6.39. 7.27, 7.84 and 8.09 N/mm^2 (using SS fibers of 0.5%, 1%, 1.5%, 2% and 2.5% respectively), when compared to FS of control specimens (at 28 days) (using plain cement mortar without SS fibers) of 5.31 N/mm^2.

2.2.2 Hybrid Reinforcement Mix

The test and control specimens of size 250 × 250 × 25 mm (thickness) have been cast (3 specimens each) as per the various combinations of mesh and fibers as shown in Table 1 and cured for 28 days. Table 1 shows three groups, GROUP 3 (3A to 3F), GROUP 4 (4A to 4F) and GROUP 5 (5A to 5F) combining 3, 4 and 5 layers of steel mesh (respectively) with SS fibers 0 to 2.5% (with 0.5% interval) in hybrid form.

Table 1. Various Reinforcing Mesh Combinations of HSMFRCC

Hybrid Steel Mesh-and-Fiber Reinforced Cementitious Composites (HSMFRCC)					
GROUP 3 Steel Mesh-3 Layers +SS-Fiber %		GROUP 4 Steel Mesh-4 Layers- +SS-Fiber %		GROUP 5 Steel Mesh-5 Layers- +SS-Fiber %	
3A	SM3L+SSF0.0	4A	SM4L+SSF0.0	5A	SM5L+SSF0.0
3B	SM3L+SSF0.5	4B	SM4L+SSF0.5	5B	SM5L+SSF0.5
3C	SM3L+SSF1.0	4C	SM4L+SSF1.0	5C	SM5L+SSF1.0
3D	SM3L+SSF1.5	4D	SM4L+SSF1.5	5D	SM5L+SSF1.5
3E	SM3L+SSF2.0	4E	SM4L+SSF2.0	5E	SM5L+SSF2.0
3F	SM3L+SSF2.5	4F	SM4L+SSF2.5	5F	SM5L+SSF2.5

Note: HSMFRCC-Hybrid Steel Mesh-and-Fiber Reinforced Cementitious Composites; SM-Steel Mesh; SS-Stainless Steel.

In Table 1, Hybrid reinforcing mix combination: SM3L+SSF 0.5, SM3L means Steel Mesh of three layers and SSF0.5 specifies that Stainless Steel-Fibers of 0.5% are used as reinforcement in cementitious matrix, and similar terminologies have been used for other combinations. The volume fraction of steel weld mesh reinforcement (V_r) has been calculated using the formula given by Naaman (2000) (p.25,26) and Shaheen *et al.* (2013) in Eq. (1) below:

$$V_r(\%) = \frac{N\pi d_w^2}{2hD} \times 100 \quad (1)$$

where, D = Grid spacing of mesh (12.5 mm, square)
d_w = diameter of mesh wire (0.7 mm)
h = Thickness of the element (25 mm)
N = no. of mesh layers (3 to 5 layers)
$V_{r(\%)}$ = Volume fraction of mesh reinforcement (in percentage)

From Eq. (1), the volume fraction of steel mesh volume of reinforcement (SM-V_r) for 3, 4 and 5 layers is calculated as 0.74%, 0.98% and 1.23% respectively.

2.2.3 Casting of Specimens

Wooden moulds were used to cast the specimens of size 250 mm × 250 mm × 25 mm (thickness). As the casting procedure is the same for control and test specimens, the terminology, 'mortar' is commonly used in places of "plain cement mortar" for control specimens and "SS-fibrous cement mortar" for test specimens.

The moulds were cleaned and placed on moisture-resistant and water-proof plywood, and oiled. First, the number of layers to be laid is marked on the moulds and base cover layer of 3 mm is laid with mortar (using 3 mm thick spacers which are removed after use). For better compaction of the matrix in reinforcing mesh and fibers, casting hand pressure was given by firmly pressing the mortar, manually using mason's trowel and finishing the layer, as shown in image (d)-Fig. 1. Now, the galvanized steel weld mesh (cut to required slab size) is then placed over the mortar, as shown in image (e)-Fig. 1. Again the mortar is laid over the first layer of mesh, as shown in image (f)-Fig. 1. At each stage, the casting pressure to the mortar is given on the cement matrix with the intention to properly pack the mesh grid spaces, reducing the voids and for densification of the cementitious matrix. After ensuring that the top levels are evenly finished, the second layer of mesh is placed over the finished surface, and the process is continued till the number of mesh layers (3, 4 or 5 layers) is laid. Finally, the top cover of 3 mm (to reinforcing mesh) is laid using the removable glass spacers, and top surface finished. Curing of the specimens is done (using gunny sacks) immediately after hardening of slab specimens for 28 days.

Fig. 2. Low-Velocity Impact Test Set-up

2.2.4 Impact Test

The impact test set-up as shown in Fig. 2 consists of a steel frame with rigid base, with rope-and-pulley arrangement. In order to conduct the low-velocity repeated drop weight test, the slab is placed on simply supported conditions on all four sides) in a separate frame with rigid base. A steel ball weighing 1 kg (9.81 N) is tied to the rope and manually raised to fixed height of 600 mm and subjected to repeated drop weight test and made to vertically fall centrally on the specimen.

During the impact testing process, there is a loss of potential energy which is accumulated in the form of absorbed energy in the materials, and dissipated as strain energy. The initial stresses are developed in the elements during the impact loading causing the first visible crack to naked eye on the bottom side of the specimen. ACI 549R (1997) describes that micro-cracks are inherent in the cement mortar matrix even before application of impact load; and as the micro-cracks widen, propagate, and progressively join together under such impact load, they are detected by some means, visual or otherwise, and termed as first crack. After carefully observing the appearance of the first crack at a particular blow, the impact test was continued till the ultimate failure stage is reached.

During the experimental programme, the number of blows which has caused the specified distress are noted down, and the energy needed to fracture the specimen are calculated using Eq. (2) of Sakthivel *et al.* (2014c), as shown below:

$$E_{imp} = n \times w \times h \quad (2)$$

where, E_{imp} = Impact Energy (Nm or J, Joules)
h = Drop height of the mass (m)
n = no. of blows
w = weight of the body (N)

The total absorbed impact energy by a single slab panel is the cumulative addition of energy absorbed during each blow until the failure. From the experimental results, the average IIEA (at first crack) and UIEA (at ultimate specimen failure) for GROUP 3 (3A to 3F), GROUP 4 (4A to 4F) and GROUP 5 (5A to 5F) are calculated and presented in Table 2.

3. Results and Discussion

3.1 Mechanical Properties

3.1.1 Impact Strength

The test results of IIEA and UIEA of GROUP 3 (SM-3L+SSF-0 to 2.5 representing 3 mesh layers and varying percentage of SS fibers), GROUP 4 (SM-4L+SSF-0 to 2.5 representing 4 mesh layers and varying percentage of SS fibers), and GROUP 5 (SM-5L+SSF-0 to 2.5 representing 5 mesh layers and varying percentage of SS fibers) are given in Table 2 and Figs. 3 and 4.

It can be observed that for GROUP 3, HSMFRCC with 3 mesh layers (V_r = 0.74%) and SS fiber V_f=0.5-2.5%, IIEA for 3B to 3F (test specimens), IIEA ranges between 29.43 J and 82.40 J respectively, when compared to 3A (control specimens) of 17.66 J, and the maximum strength improvement is observed for 3F with Strength Improvement Ratio (SIR) of 4.67. The UIEA for

Table 2. Experimental Results of Impact Tests of HSMFRCC

TYPE	IIEA (Joules)	SIR	t test	UIEA (Joules)	SIR	t test
GROUP 3 (3 nos. of Steel Mesh Layers + Varying SS Fiber 0-2.5%)						
3A (CS)	17.66	--	t=5.00 p<0.01 (N=6)	406.13	--	t=10.56 p<0.01 (N=6)
3B (TS)	29.43	1.67		459.11	1.13	
3C (TS)	41.20	2.33		529.74	1.30	
3D (TS)	58.86	3.33		600.37	1.48	
3E (TS)	64.75	3.67		671.00	1.65	
3F (TS)	82.40	4.67		759.29	1.87	
	Average SIR	3.13		Average SIR	1.49	
GROUP 4 (4 nos. of Steel Mesh Layers + Varying SS Fiber 0-2.5%)						
4A (CS)	41.20	--	t=7.23 p<0.01 (N=6)	635.69	--	t=14.12 p<0.01 (N=6)
4B (TS)	52.97	1.29		671.00	1.06	
4C (TS)	64.75	1.57		759.29	1.19	
4D (TS)	76.52	1.86		847.58	1.33	
4E (TS)	94.18	2.29		918.22	1.44	
4F (TS)	105.95	2.57		988.85	1.56	
	Average SIR	1.92		Average SIR	1.32	
GROUP 5 (5 nos. of Steel Mesh Layers + Varying SS Fiber 0-2.5%)						
5A (CS)	64.75	--	t=9.80 p<0.01 (N=6)	1059.48	--	t=25.26 p<0.01 (N=6)
5B (TS)	76.52	1.18		1094.80	1.03	
5C (TS)	88.29	1.36		1147.77	1.08	
5D (TS)	94.18	1.45		1218.40	1.15	
5E (TS)	111.83	1.73		1289.03	1.22	
5F (TS)	129.49	2.00		1359.67	1.28	
	Average SIR	1.54		Average SIR	1.15	

HSMFRCC-Hybrid Steel Mesh-and-Fiber Reinforced Cementitious Composites; IIEA-Initial Impact Energy Absorption; UIEA-Ultimate Impact Energy Absorption; CS-Control Specimens (SMRCC-Steel Mesh Reinforced Cementitious Composites), TS-Test Specimens (HSMFRCC-Hybrid Steel Mesh-and-Mesh Reinforced Cementitious Composites); SIR-Strength Improvement Ratio; N-No. of Samples for one-sample test.

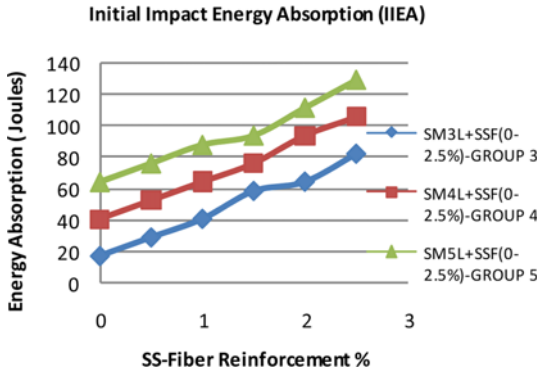

Fig. 3. IIEA of HSMFRCC

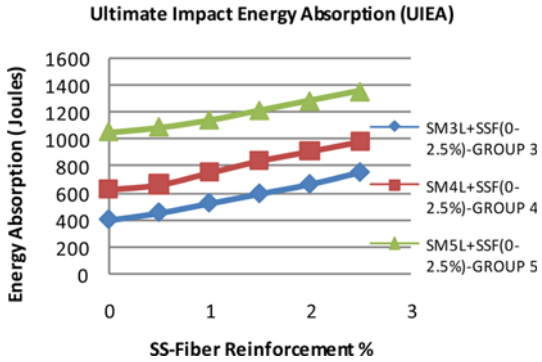

Fig. 4. UIEA of HSMFRCC

GROUP 3 (3B to 3F) ranges from 459.11 J to 759.29 J respectively, when compared to 3A of 406.13 J, with SIR of 1.87 for 3F demonstrating maximum strength improvement of 86.96%, when SS fiber V_f = 2.5% is used.

Similarly, for GROUP 4 - HSMFRCC with 4 mesh layers (V_r = 0.98%) and SS fiber V_f = 0.5-2.5%, IIEA for 4B to 4F varied between 52.97 J and 105.95 J respectively, when compared to 4A of 41.20 J. The maximum IIEA strength improvement is seen for 4F with SIR of 2.57. The UIEA for GROUP 4 (4B to 4F) ranges from 671.00 J to 988.85 J, when compared to 4A of 635.69 J showing SIR of 1.56 for 4F indicating maximum strength improvement of 55.55%, when SS fiber V_f = 2.5% is used.

And for GROUP 5 - HSMFRCC with 5 mesh layers (V_r = 0.98%) and varying SS fiber V_f = 0-2.5%, IIEA for 5B to 5F varied between 76.52 J and 129.49 J when compared to 5A of 64.75 J, and the maximum IIEA strength improvement is obtained for 5F with SIR of 2.00. The UIEA for GROUP 5 (5B to 5F) ranges from 1094.80 J to 1359.67 J, when compared to 5A of 1059.480 J showing SIR of 1.28 for 5F representing maximum strength improvement of 28.33%, when SS fiber V_f = 2.5% is used.

It is inferred from the results in Table 2 and Figs. 3 and 4 that when steel mesh layer (3 or 4 or 5 layers) is kept constant in each group (GROUPS 3, 4 and 5), and SS fibers varied, there is increase in impact energy absorption of slabs.

From Table 2, the average strength improvement ratio (SIR) for GROUPS 3, 4 and 5 of 3.13, 1.92 and 1.54 for IIEA and 1.49, 1.32 and 1.15 for UIEA (respectively) shows that the impact strength reduces as the mesh and fiber volume percentage reinforcement is increased, this might be probably due to more congestion of reinforcement. Also, when the UIEA results of the present study of 759.29 J, 988.85 J and 1359.67 J (for 3F, 4F and 5F) corresponding to varying steel mesh layers of 3, 4 and 5 steel mesh layers with stainless steel fibers of 2.5% respectively is compared to the UIEA results of Sakthivel *et al.* (2014c) of 1783.46 J, 2366.17 J and 3407.99 J who have used varying 3, 4 and 5 steel mesh layers and polyolefin fibers of 2.5%, the impact strength performance of SS fibers is found to be only about 41% of polyolefin fibers in cementitious matrix.

3.1.2 One Sample Tests

One-sample test is conducted to find whether there is any significant difference in the energy absorption capacity of slabs (Sakthivel *et al.*, 2014c) when SS fiber volume fraction (SSF-V_f) of 0-2.5% (with 0.5% interval) in GROUPS 3, 4 and 5, keeping Steel Mesh-Volume of reinforcement (SM-V_r) of 0.74%, 0.98% and 1.23% constant in their respective groups, and the results given in Table 2.

From Table 3, one sample test for IIEA under GROUPS 3, 4 and 5 shows t = 5.00 ($p<0.01$), t = 7.23 ($p<0.01$) and t = 9.80 ($p<0.01$) implies that there is a significant difference in IIEA values when SS fiber percentage (SS-Vf) is varied (0, 0.5%, 1%, 1.5%, 2% and 2.5%), and keeping mesh layers (3,4,5) constant in all the three groups, GROUPS 3, 4 and 5. Similarly, one sample test for UIEA shows t = 10.56 ($p<0.01$), t = 14.120 ($p<0.01$) and t = 25.26 ($p<0.01$) respectively. This means that when SS fibers is increased from 0 to 2.5% (with 0.5% interval) (while keeping the steel mesh layers constant), there has been significant positive increase in the impact values in IIEA and UIEA in all the three groups, GROUPS 3, 4 and 5.

3.1.3 Paired t-Tests

From the experimental test results of IIEA and UIEA of 18 combinations under all the three groups (GROUPS 3, 4 and 5) in Table 2, paired t-tests are conducted and presented in Table 3. From Table 3, Pair 1, it can be seen that paired t-test has been conducted to find out whether there is any significant difference between the impact energy absorption at first crack and ultimate failure stages. It was observed from Table 3 that Pair No.1 of

Table 3. Paired t-Tests on various Groups of IIEA and UIEA

Pair No.	Pairing Variables	N	R	t	df
1	IIEA & UIEA	18	0.893	12.553*	17
2	IIEA-GROUPS 3 & 4	6	0.989	15.495*	5
3	IIEA-GROUPS 4 & 5	6	0.993	17.380*	5
4	IIEA-GROUPS 3 & 5	6	0.980	23.008*	5
5	UIEA-GROUPS 3 & 4	6	0.997	42.835*	5
6	UIEA-GROUPS 4 & 5	6	0.996	36.851*	5
7	UIEA-GROUPS 3 & 5	6	0.998	83.746*	5

R-Multiple Correlation Co-efficient; N=No. of Pairs, *Sig. at $p<0.01$.

IIEA-UIEA shows a good correlation value of R = 0.893 ($p<0.01$) with t = 12.553 ($p<0.01$) demonstrating that there is statistically significant difference in impact values between IIEA and UIEA in all 18 types.

Further, paired t-test is conducted to find out whether there is any significant difference in IIEA in Pair 2 (between GROUPS 3 and 4), Pair 3 (GROUPS 4 and 5) and Pair 4 (between GROUPS 3 and 5) and the results are presented in Table 3. The three pairs (pair no. 2, 3, 4) show R values of 0.989, 0.993 and 0.980 demonstrating high level of correlation in IIEA between GROUPS 3 and 4, 4 and 5, and 3 and 5 respectively. Further, the values of t = 15.495 ($p<0.01$), t = 17.380 ($p<0.01$) and 23.008 ($p<0.01$) respectively shows that there is significant positive increase in IIEA between any two groups, GROUPS 3 and 4, GROUPS 4 and 5, and GROUPS 3 and 5, when the mesh layers are increased from 3 to 4, 4 to 5 and 3 to 5 layers respectively, when SS-V_f = 0 to 2.5%.

Similarly, in pairs 5, 6 and 7, paired t-tests show R values of 0.997, 0.996 and 0.998 showing high level of correlation in UIEA between GROUPS 3 and 4, 4 and 5, and 3 and 5 respectively. Also, the values of t = 42.835 ($p<0.01$), t = 36.851 ($p<0.01$) and 83.746 ($p<0.01$) bring out that there is significantly positive increase in ultimate impact values between any two groups, GROUPS 3 and 4, GROUPS 4 and 5, and GROUPS 3 and 5 respectively when the mesh layers are increased from 3 to 4, 4 to 5 and 3 to 5 respectively and SS-V_f from 0 to 2.5%.

Table 4. Predicted and Experimental Results of IIEA

Type	No. of Steel Mesh Layers SM-Vr% in bracket	IIEA (Exp.) (in Joules)	IIEA Strength Improvement Ratio (SIR)		IIEA (Pred.) (in Joules)	Pred. Error
CONTROL SPECIMENS (SMRCC)						
SS FIBERS-0.0%						
3A	3(0.74)	17.66	2.33		17.59	-0.40
4A	4(0.98)	41.20		1.57	39.67	-3.86
5A	5(1.23)	64.75			62.68	-3.30
TEST SPECIMENS (HSMFRCC)						
SS FIBERS-0.5%						
3B	3(0.74)	29.43	1.80		30.37	+3.19
4B	4(0.98)	52.97		1.44	52.46	-0.97
5B	5(1.23)	76.52			75.47	-1.39
SS FIBERS-1.0%						
3C	3(0.74)	41.20	1.57		43.15	+4.73
4C	4(0.98)	64.75		1.36	65.24	+0.76
5C	5(1.23)	88.29			88.25	-0.05
SS FIBERS-1.5%						
3D	3(0.74)	58.86	1.30		55.93	-5.24
4D	4(0.98)	76.52		1.23	78.02	+1.96
5D	5(1.23)	94.18			101.03	+7.27
SS FIBERS-2.0%						
3E	3(0.74)	64.75	1.45		68.71	+6.12
4E	4(0.98)	94.18		1.19	90.80	-3.72
5E	5(1.23)	111.83			113.81	+1.77
SS FIBERS-2.5%						
3F	3(0.74)	82.40	1.29		81.50	-1.10
4F	4(0.98)	105.95		1.22	103.58	-2.29
5F	5(1.23)	129.49			126.59	-2.29
	Average IIEA-SIR (for test specimens)		1.48	1.29		

UIEA-Initial Impact Energy Absorption; CS-Control Specimens (SMRCC-Steel Mesh Reinforced Cementitious Composites); TS-Test Specimens (HSMFRCC-Hybrid Steel Mesh-and-Fiber Reinforced Cementitious Composites), Exp.-Experimental Results; Pred.-Predicted Values; SII - Strength Improvement Ratio.

3.2 Statistical Analysis

3.2.1 Strength Improvement

The Strength Improvement Ratio (SIR) of IIEA and UIEA values are presented in Tables 4 and 5. From Table 4, it can be seen that when the volume percentage of SS fiber is kept constant (SS-V_f = 0%, 0.5%, 1.0%, 1.5%, 2% and 2.5%) and steel mesh layers increased from 3 to 4 nos. and 4 to 5 nos., there is an increase in IIEA of control specimens by 2.33 and 1.57 times (respectively), and test specimens (average of all specimens) by 1.48 and 1.29 times (respectively).

Similarly, from Table 5, it is seen that when the volume percentage of SS fiber is kept constant (SS-V_f= 0%, 0.5%, 1.0%, 1.5%, 2% and 2.5%), and steel mesh layers varied from 3 to 4 layers and 4 to 5 layers, there is an increase in UIEA of control specimens by 1.56 and 1.67 times (respectively), and test specimens (average of all specimens) by 1.39 and 1.47 times (respectively).

3.2.2 Prediction Models

In order to develop prediction models, regression analysis have been used between the dependent and independent variables, considering IIEA/ UIEA as the dependent variable, and mesh volume fraction of reinforcement (SM-V_r) of 0.74%, 0.98% and 1.23% (corresponding to 3, 4 and 5 layers galvanized steel mesh) and stainless steel volume fraction (SSF-V_f) of 0-2.5% as the independent variables. The multiple regression analysis is employed to formulate the predictive equations linking the dependent variable (IIEA or UIEA) and independent variables (steel mesh volume of reinforcement, SM-V_r and steel fiber volume fraction, SSF-V_f) using the experimental data and ANOVA results to illustrate the effect that the variables have on one another (Sahmaran *et al*., 2013).

The square of the correlation (co-efficient of determination, R^2), which is the measure of the proportion of the variance of the dependent variable about its mean is explained by the independent (or predictor) variable. The coefficient can vary between 0 and 1, where closer to one suggest a more accurate model. Thus, higher the value of R^2, the greater the explanatory power of the regression equation and therefore better is the prediction level of dependent variable.

Based on the experimental results in Tables 4 and 5, statistical prediction models for IIEA and UIEA are derived using statistical regression analysis, and presented in Tables 6 and 7 respectively. The predicted values calculated from the predicted models are

Table 5. Predicted and Experimental Results of UIEA

Type	Steel Mesh Layers SMVr% in bracket	UIEA (Exp.) (in Joules)	UIEA Strength Improvement Ratio (SIR)		UIEA (Pred.) (in Joules)	Pred. Error
CONTROL SPECIMENS (SMRCC)						
SS FIBERS-0.0%						
3A	3(0.74)	406.13	1.56		374.13	-8.55
4A	4(0.98)	635.69		1.67	680.21	+7.00
5A	5(1.23)	1059.48			999.04	-6.05
TEST SPECIMENS (HSMFRCC)						
SS FIBERS-0.5%						
3B	3(0.74)	459.11	1.46		442.91	-3.66
4B	4(0.98)	671.00		1.63	748.99	+11.62
5B	5(1.23)	1094.80			1067.82	-2.53
SS FIBERS-1.0%						
3C	3(0.74)	529.74	1.43		511.69	-3.53
4C	4(0.98)	759.29		1.51	817.77	+7.70
5C	5(1.23)	1147.77			1136.60	-0.98
SS FIBERS-1.5%						
3D	3(0.74)	600.37	1.41		580.47	-3.42
4D	4(0.98)	847.58		1.44	886.55	+4.60
5D	5(1.23)	1218.40			1205.38	-1.08
SS FIBERS-2.0%						
3E	3(0.74)	671.00	1.37		649.26	-3.35
4E	4(0.98)	918.22		1.40	955.33	+4.04
5E	5(1.23)	1289.03			1274.17	-1.17
SS FIBERS-2.5%						
3F	3(0.74)	759.29	1.30		718.04	-5.74
4F	4(0.98)	988.85		1.37	1024.12	+3.57
5F	5(1.23)	1359.67			1342.95	-1.24
	Average IIEA-SIR (for test specimens)		1.39	1.47		

UIEA-Initial Impact Energy Absorption; CS-Control Specimens (SMRCC-Steel Mesh Reinforced Cementitious Composites); TS-Test Specimens (HSMFRCC-Hybrid Steel Mesh-and-Fiber Reinforced Cementitious Composites), Exp.-Experimental Results; Pred.-Predicted Values; SIR - Strength Improvement Ratio.

compared with the experimental results, and the predicted error between the predicted and experimental values for IIEA and UIEA are shown in Tables 4 and 5. The statistical regression analysis presented in Tables 6 and 7 shows high R value of 0.996 and 0.991 for IIEA and UIEA respectively demonstrating higher levels of correlation between the dependent variable (IIEA or UIEA) and the independent variables (SSF-Vf and SM-Vr). Also, the R^2 value of 0.992 and 0.983 for IIEA and UIEA (respectively) closer to 1 is highly desirable and also gives a picture of reliable confidence in the estimation of response efficiencies (Aldahdooh *et al*., 2014); and also adequately fit the experimental data with a $p<0.01$, explaining the variability of 99.2% and 98.3% of SM-V_r and SSF-V_f for IIEA and UIEA models. Thus, these two variables SM-V_r and SSF-V_f have significantly contributed to both the models (as in Tables 6 and 7) with 99% confidence level (Sahmaran *et al.*, 2013).

Also from Tables 6 and 7, it can be seen that The *F* values for

Table 6. Predicted Model for IIEA of HSMFRCC

Variables	Regression Coefficient	R	R^2	F
Intercept	-50.524	0.996	0.992	945.484*
SM-V_r	92.040			
SSF-V_f	25.564			

Predicted Regression Equation for IIEA = -50.524 + 92.040 SM-V_r + 25.564 SSF-V_f (in Joules)

Note: SM-V_r = Steel Mesh Volume of Reinforcement; SSF-V_f = Stainless Steel Fiber Volume fraction; *Sig.at $p<0.01$.

Table 7. Predicted Model for UIEA of HSMFRCC

Variables	Regression Coefficient	R	R^2	F
Intercept	-569.613	0.991	0.983	426.327*
SM-V_r	1275.327			
SSF-V_f	137.564			

Predicted Regression Equation for IIEA = -569.613 + 1275.327 SM-V_r + 137.564 SSF-V_f (in Joules)

Note: SM-V_r = Steel Mesh Volume of Reinforcement; SSF-V_f = Stainless Steel Fiber Volume fraction; *Sig.at $p<0.01$.

IIEA and UIEA models of the regression are found to be 945.484 ($p<0.01$) and 426.307 ($p<0.01$) respectively and accepted as the significant models (Sahmaran *et al*., 2013).

From Tables 4 and 5, it can be seen that the prediction error between the experimental and predicted values for IIEA ranges between -5.23% and +7.28% and for UIEA between -8.55% and +11.62%, which is within the permissible limit of variation of 15%. The absolute average predicted error percentage for IIEA and UIEA are 2.8% and 4.43%, which is within the acceptable levels of 10%. As the prediction models are as close as possible to real system within tolerable limits, both the IIEA and UIEA predicted equations can be used as reliable models for determining the impact strength of HSMFRCC. The process of validation of the predicted models (in Tables 6 and 7) are presented in Section 3.2.3.

3.2.3 Validation of Predicted Models

In order to validate the predicted regression models for IIEA and UIEA given in Tables 6 and 7 respectively, 3 slabs were cast of the same dimensions, 250 mm × 250 mm × 25 mm (thickness) as per the procedure given in Section 2.2.3 The SS-fibrous cement mortar specimens with SS fibers of 1.75% (of volume of specimens) using sand-cement ratio 2:1 and water-cement ratio of 0.43 has given 28 days compressive strength of 34.82 N/mm^2,

Table 8. Validation of Predicted Models

Predicted Models	Predicted Value (J)	Experimental Value (J)	Error (%)
IIEA (J) = -50.524 + (92.040 × SM-V_r) + (25.564 SSF-V_f)	84.41	88.29	-4.60
UIEA (J) = -569.613 + (1275.327 × SM-V_r) + (137.564 × SSF-V_f)	920.94	894.67	+2.94

Note: SM-V_r = Steel Mesh Volume of Reinforcement; SM-Vr = 0.98 (for 4 mesh layers); SSF-V_f = Stainless Steel Fiber Volume fraction, J-Joules, SSF-V_f = 1.75; IIEA-Initial Impact Energy Absorption, UIEA-Ultimate Impact energy.

split-tensile strength of 7.32 N/mm^2 and prismatic beam flexural strength of 7.52 N/mm^2.

The impact testing procedure as given in Section 2.2.4 is repeated for the newly cast specimens. The predicted values for IIEA and UIEA are arrived from the regression equations (from Tables 6 and 7), using the new reinforcement combinations are 84.41 J and 920.94 J respectively and presented in Table 8. The new experimental impact values for IIEA and UIEA (average of 3 specimens) show 88.29 J and 894.67 J respectively, which are presented in Table 8. The error between the predicted and experimental values for the new specimens are found to be -4.60% for IIEA and +2.94% for UIEA, and the variations are very low and within the prescribed limits of 15%. Hence the models are validated and can be reliably used to determine the impact strength of HSMFRCC.

4. Conclusions

Steel Mesh Reinforced Cementitious Composites (SMRCC) has its limitations of element thickness and number of mesh layers and Fiber Reinforced Cementitious Composites (FRCC) has constraints in using fiber beyond 2.5%. Therefore, this study has employed an hybrid technique of integrating steel mesh with SS fibers as reinforcement in cementitious composites.

This paper has experimentally investigated the impact resistance of Hybrid Steel Mesh-and-Fiber Reinforced Cementitious Composites (HSMFRCC) using 3, 4 and 5 layers (SM-Vr of 0.74%, 0.98% and 1.23% respectively) and stainless steel fiber (SSF-Vf) of 0.5-2.5%, and following are the concluding remarks:

1. It was seen that when the number of steel mesh layers are increased from 3 to 4, and 4 to 5, keeping SS fiber percentage constant in cementitious composites, the impact values (on an average) has increased for Initial Impact Energy Absorption (IIEA) by about 1.48 and 1.29 times respectively, and Ultimate Impact Energy Absorption (UIEA) by about 1.39 and 1.47 times respectively.
2. When the stainless steel fibers are increased from 0 to 2.5% and 3, 4 and 5 steel mesh layers are kept constant, the IIEA has increased atleast 3.13, 1.92 and 1.54 times and UIEA 1.49, 1.32 and 1.15 times (with respect to control specimens) when 3,4 and 5 mesh layers are used. But a downward trend in the average Strength Improvement Ratio (SIR) values is seen when mesh and fiber reinforcement ratios are jointly increased.
3. The statistical models developed for initial and ultimate impact strength in this study are validated, which is capable of accurately predicting the impact energy absorption capacity of hybrid mesh-and-fiber reinforced cementitious composite slab elements. This will certainly help the researchers and construction practitioners to predict the impact strength of such composites before actual application in the field.
4. It is also recommended that experimental investigation on flexural behavior of hybrid mesh and fiber reinforced cementitious slab elements be conducted to determine the flexural toughness and deflection ductility characteristics.

Acknowledgements

The corresponding author, P.B. Sakthivel, Ph.D. Research Scholar in Civil Engineering (Part time- External), Pondicherry Engineering College (P.E.C.), Puducherry, India, and Associate Professor of Civil Engineering, Agni College of Technology, Chennai, India thank Prof. Dr. D. Govindarajalu, Principal, P.E.C. for providing valuable suggestions for this research.

References

ACI 544 (1998). *State-of-the-art report on fiber reinforced concrete*, ACI Committee, USA.

ACI 549R (1997). *State-of-the-art report on ferrocement,* ACI Committee, USA.

Aldahdooh, M. A. A., Bunnori, N. M., and Johari, M. A. M. (2014). "Influence of palm oil fuel ash on ultimate flexural and uniaxial tensile strength of green ultra-high performance fiber reinforced cementitious composites." *Materials and Design*, Vol. 54, pp. 694-701, DOI: 10.1016/j.matdes.2013.08.094.

Aldousiri, B., Alajmi, M., and Shalwan, A. (2013). "Mechanical properties of palm fibre reinforced recycled HDPE." *Advances in Materials Science and Engineering*, Vol. 2013, DOI: 10.1155/2013/508179.

Al-Hadithi, A. I. and Al-Nu'man, B. S. (2008). "Behavior of polymer modified concrete slabs under impact." *Iraqi Journal of Civil Engineering,* Vol. 5, No. 11, pp. 1-24.

Almusallam, T. H., Siddiqui, N. A., Iqbal, R. A., and Abbas, H. (2013). "Response of hybrid-fiber reinforced concrete slabs to hard projectile impact." *International Journal of Impact Engineering*, Vol. 58, pp. 17-30, DOI: 10.1016/j.ijimpeng.2013.02.005.

Cachim, P., Velosa, A. L., and Ferraz, E. (2014). "Substitution Materials for sustainable concrete production in Portugal." *KSCE Journal of Civil Engineering*, KSCE, Vol. 18, No. 1, pp. 60-66, DOI: 10.1007/s12205-014-0201-3.

Cavdar, A. (2014). "Investigation of freeze-thaw effects on mechanical properties of fiber reinforced cement mortars." *Composites: Part B*, Vol. 58, March, pp. 463-472, DOI: 10.1016/j.compositesb.2013.11.013.

Cheah, C. B. and Ramli, M. (2012). "Load capacity and crack development characteristics of HCWA-DSF high strength mortar ferrocement panels in flexure." *Construction and Building Materials*, Vol. 36, November, pp. 348-357, DOI: 10.1016/j.conbuildmat.2012. 05.034.

Colombo, M., di Prisco, M., and Felicetti, R. (2010). "Mechanical properties of steel fibre reinforced concrete exposed at high temperatures." *Materials and Structures*, Vol. 43, No. 4, pp. 475-491, DOI: 10.1617/s11527-009-9504-0.

Elavenil, S. and Knight, G. M. S. (2012). "Impact response of plates under drop weight impact testing." *Daffodil International University Journal of Science and Technology*, Vol. 7, No. 1, pp. 1-11, DOI: 10.3329/diujst.v7i1.9580.

Farnam, Y., Mohammadi, S., and Sherkarchi, M. (2010). "Experimental and numerical investigations of low velocity impact behavior of high performance fiber-reinforced cement based composite." *International Journal of Impact Engineering*, Vol. 37, No. 2, pp.

220-229, DOI: 10. 116/j.ijimpeng.2009.08.006.

Holschemacher, K., Mueller, T., and Ribakov, Y. (2010). "Effect of steel fibers on mechanical properties of high-strength concrete." *Materials and Design*, Vol. 31, No. 5, pp. 2604-2615, DOI: 10.1016/j.matdes. 2009.11.025.

Ibrahim, H. M. (2011). "Experimental investigation of ultimate capacity of wire mesh-reinforced cementitious slabs." *Construction and Building Materials*, Vol. 25, No. 1, pp. 251-259, DOI: 10.1016/j. conbuildmat.2010.06.032

IS 12269-1987 (2008). *Specification for 53 grade ordinary Portland Cement*, Bureau of Indian Standards, New Delhi, India

IS:383-1987 (2007). *Specification for coarse and fine aggregates from natural sources for concrete*, Bureau of Indian Standards, New Delhi, India.

Kaleemulla, K. M. and Siddeswarappa, B. (2011). "Low velocity impact fatigue studies on hybrid composite laminates with varied material and test parameters - Effect of impact energy and fibre volume fraction." *International Journal of Structural Engineering*, Vol. 2, No. 1, pp. 1-12. DOI: 10.1504/IJStructE.2011.038065.

Kim, D. J., Naaman, A. E., and El-Tawil, S. (2008). "Comparative flexural behavior of four fiber reinforced cementitious composites." *Cement and Concrete Composites*, Vol. 30, No. 10, pp. 917-928, DOI: 10.1016/j.cemconcomp.2008.08.002.

Kuder, K. G., Mu, E. B., and Shah, S. P. (2006). "New method to evaluate the nailing performance of extruded high-performance fiber-reinforced cementitious composites for residential applications." *Journal of Materials in Civil Engineering*, ASCE, Vol. 18 No. 3, pp. 443-452, DOI: 10.1061/(ASCE)0899-1561(2006)18:3 (443).

Lin, V. W. J., Quek, S. T., and Maalej, M. (2011). "Static and dynamic tensile behaviour of PE-fibrous ferrocement." *Magazine of Concrete Research*, Vol. 63, No. 1, pp. 61-73, DOI: 10.1680/macr.2011.63.1.61.

Maalej, M., Quek, S. T., and Zhang, J. (2005). "Behavior of hybrid-fiber engineered cementitious composites subjected to dynameic tensile loading and projectile impact." *Journal of Materials in Civil Engineering*, ASCE, pp. 143-152, DOI: 10.1061/(ASCE)0899-1561 (2005)17:2(143).

Mo, K. H., Yap, S. P., Alengaram, U. J., Jumaat, M. Z., and Bu, C. H. (2014). "Impact resistance of hybrid fiber-reinforced oil palm shell concrete." *Construction and Building Materials*, Vol. 50, pp. 499-507, DOI: 10.1016/j.conbuildmat.2013.10.016.

Mohammed, A. A. and Assi, D. K. (2011). "Tensile stress-strain relationship for ferrocement structures." *Al-Rafidain Engineering*, Vol. 20, No. 2, pp. 27-40, http://www.iasj.net/iasj?func=fulltext& aId=47274.

Molero, M., Segura, I., Hernandez, M. G., Izquierdo, M. A. G., and Anaya, J. J. (2011). "Ultrasonic wave propagation in cementitious materials: A multiphase approach of a self-consistent multiple scattering model." *Ultrasonics*, Vol. 51 No. 1, pp. 71-84, DOI: 10. 1016/ j.ultras.2010.06.001.

Naaman, A. E. (2000). "Ferrocement & laminated cementitious composites." *Techno Press 3000*, Ann Arbor, Michigan 48105, USA.

Narendar, R., Dasan, K. P., and Nair, M. (2014). "Development of coir pith/nylon fabric/epoxy hybrid composites: Mechanical and ageing studies." *Materials and Design*, Vol. 54, pp. 644-651, DOI: 10.1016/ jmatdes.2013.08.080.

Ong, K. C. G., Basheerkhan, M., and Paramasivam, P. (1999). "Resistance to fibre concrete slabs to low velocity projectile impact." *Cement & Concrete Composites*, Vol. 21, No. 5, pp. 391-401.

Peled, A. and Shah, S. P. (2003). "Processing effects in cementitious composites: Extrusion and casting." *Journal of Materials in Civil Engineering,* ASCE, Vol. 15 No. 2, pp. 192-199, DOI: 10.1061/ (ASCE)0899-1561(2003)15:2(192).

Pereira, E. B., Fischer, G., and Barros, J. A. O. (2012). "Effect of hybrid fiber reinforcement on the cracking process in fiber reinforced cementitious composites." *Cement & Concrete Composites*, Vol. 34, No. 10, pp. 1114-1123, DOI: 10.1016/j.cemconcomp.2012.08.004.

Pereira, C. L., Savastano Jr., H., Paya, J., Santos, S. F., Borrachero, M. V., Monzo, J., and Soriano, L. (2013). "Use of highly reactive rice husk ash in the production of cement matrix reinforced with green coconut fiber." *Industrial Crops and Products*, Vol. 49, pp. 88-96, DOI: 10.1016/j.indcrop.2013.04.038.

Ramasamy, V. (2012). "Compressive strength and durability properties of rice husk ash concrete." *KSCE Journal of Civil Engineering*, KSCE, Vol. 16, No. 1, pp. 93-102, DOI: 10.1007/s12205-012-0779-2.

Rambo, D. A. S., Silva, F. A., and Filho, R. D. T. (2014). "Mechanical Behavior of hybrid steel-fiber self-consolidating concrete: Materials and structural aspects." *Materials and Design*, Vol. 54, pp. 32-42, DOI: 10.1016/j.matdes.2013.08.014.

Ren, F., Mattus, C. H., Wang, J. J., and DiPaolo, B. P. (2013). "Effect of projectile impact and penetration on the phase composition and microstructure of high performance concretes." *Concrete & Concrete Composites*, Vol. 41,pp. 1-8, DOI: 10.1016/j.cemconcomp. 2013. 04.007.

Sahmaran, M., Bilici, Z., Ozhay, E., Erden, T. K., Yucel, H. E., and Lachemi, M. (2013). "Improving the workability and rheological properties of engineered cementitious composites using factorial experimental design." *Composites: Part B*, Vol. 45, No. 1, pp. 356-368, DOI: 10.1016/j.compositesb.2012.08.015.

Sakthivel, P. B. and Jagannathan, A. (2012a). "Compatibility study of PVC-coated weld mesh in thin reinforced cementitious matrix." *Proceedings of the 10th International Symposium on Ferrocement and Thin Reinforced Cement Composites (FERRO-10)*, Havana, Cuba, pp. 17-27.

Sakthivel, P. B. and Jagannathan, A. (2012b). "Corrosion-free cementitious composites for sustainability." *Proceedings of the 37th Conference on Our World in Concrete & Structures,* Singapore, pp. 1-13, http:// www.cipremier.com/100037036.

Sakthivel, P. B., Jagannathan, A., and Padmanaban, R. (2012). "Thin cementitious slabs reinforced with stainless steel fibers." *IOSR Journal of Mechanical and Civil Engineering (IOSR-JMCE)*, Vol. 4, No. 2, pp. 39-45, DOI: 10.9790/1684-0423945.

Sakthivel, P. B., Ravichandran, A., and Alagumurthi, N. (2014a). "Strength modeling of mechanical strength of polyolefin fiber reinforced cementitious composites." *KICEM Journal of Construction Engineering and Project Management*, Vol. 4, No. 2, pp. 41-46, DOI: 10.6106/JCEPM.2014.4.2.041.

Sakthivel, P. B., Ravichandran, A., and Alagumurthi, N. (2014b). "Experimental and predictive mechanical strength of fiber reinforced cementitious matrix." *International Journal of GEOMATE*, Japan, Vol. 7, No. 1, (Sl. No. 13), pp. 993-1002.

Sakthivel, P. B., Ravichandran, A., and Alagumurthi, N. (2014c). "An experimental study of mesh-and-fiber reinforced cementitious composites." *Concrete Research Letters*, Vol. 5, No. 1, pp. 722-739.

Sakulich, A. R. (2011). "Reinforced geopolymer composites for enhanced material greenness and durability." *Sustainable Cities and Society*, Vol. 1, No. 4, pp. 195-210, DOI: 10.1016/j.scs.2011.07.009.

Sayed-Ahmed, M. (2012). "Statistical modelling and prediction of compressive strength of concrete." *Concrete Research Letters*, Vol. 3, No. 2, pp. 452-458.

Shaikh, F. U. A. (2013). "Deflection hardening behaviour of short fibre

reinforced fly ash based geopolymer composites." *Materials and Design*, Vol. 50, September, pp. 674-682, DOI: 10.1016/j.matdes.2013.03.063.

Shaheen, Y. B. I., Soliman, N. M., and Kandil, D. E. M. (2013). "Influence of reinforced ferrocement concrete plates under impact load." *International Journal of Current Engineering and Technology*, Vol. 3, No. 4, http://inpressco.com/category/ijcet.

Shannag, M. J. (2008). "Bending behavior of ferrocement plates in sodium and magnesium sulfates solutions." *Cement & Concrete Composites*, Vol. 30, No. 7, pp. 597-602, DOI: 10.1016/j.cemconcomp.2008.03.003.

Shannag, M. J. and Ziyyad, T. B. (2007). "Flexural response of ferrocement with fibrous cementitious matrices." *Construction and Building Materials*, Vol. 21, No. 6, pp. 1198-1205, DOI: 10.1016/j.conbuildmat.2006.06.021.

Soe, K. T., Zhang, Y. X., and Zhang, L. C. (2013). "Impact resistance of hybrid-fiber engineered cementitious composite panels." *Composite Structures*, Vol. 104, pp. 320-330, DOI: 10.1016/j.compstruct.2013. 01.029.

Sonebi, M. and Bassuoni, M. T. (2013). "Investigating the effect of mixture design parameters on pervious concrete by statistical modelling." *Construction and Building Materials*, Vol. 38, pp. 147-154, DOI: 10.1016/j.conbuildmat.2012.07.044.

Suthiwarapirak, P., Matsumoto, T., and Kanda, T. (2004). "Multiple cracking and fiber bridging characteristics of engineered cementitious composites under fatigue flexure." *Journal of Materials in Civil Engineering*, Vol. 16, No. 5, pp. 433-443, DOI: 10.1061/(ASCE)0899-1561(2004)16:5(433).

Tabatabaei, Z. S., Volz., J. S., Keener, D. I., and Gliha, B. P. (2014). "Comparative impact behavior of four long carbon fiber reinforced concretes." *Materials and Design*, Vol. 55, pp. 212-223, DOI: 10.1016/j.matdes.2013.09.048.

Tassew, S. T. and Lubell, A. S. (2014). "Mechanical properties of glass fiber reinforced ceramic concrete." *Construction and Building Materials*, Vol. 51, pp. 215-224, DOI: 10.1016/j.conbuildmat. 2013.10.046.

Tosun-Felekoglu, K. and Felekoglu, B. (2013). "Effects of fibre hybridization on multiple cracking potential of cement-based composites under flexural loading." *Construction and Building Materials*, Vol. 41, pp. 15-20, DOI: 10.1016/j.conbuildmat.2012.09. 115.

Trainor, K. J., Foust, B. W., and Landis, E. N. (2013). "Measurement of energy dissipation mechanisms in fracture of fiber-reinforced ultrahigh strength cement-based composites." *Journal of Engineering Mechanics (ASCE),* Vol. 139, No. 7, pp. 771-779, DOI: 10.1061/(ASCE)EM.1943-7889.0000545.

Xin, L., Jin-yu, X., Er-lei, B., and Weimin, L. (2014). "Mechanical properties of ceramics-cement based porous material under impact loading." *Materials and Design*, Vol. 55, pp. 778-784, DOI: 10.1016/j.matdes.2013.10.046.

Yang, E. and Li, V. C. (2012). "Tailoring engineered cementitious composites for impact resistance." *Cement and Concrete Research*, Vol. 42, No. 8, pp. 1066-1071, DOI: 10.1016/j.cemconres.2012.04.006.

Yardim, Y., Waleed, A. M. T., Jaafar, M. S., and Laseima, S. (2013). "AAC-concrete light weight precast composite floor slab." *Construction and Building Materials*, Vol. 40, pp. 405-410, DOI: 10.1016/j.conbuildmat.2012.10.011.

Yu, R., Spiesz, P., and Brouwers, H. J. H. (2014). "Mix design and properties assessment of Ultra-High Performance Fibre Reinforced Concrete (UHPFRC)." *Cement and Concrete Research*, Vol. 56, pp. 29-39, DOI: 10.1016/j.cemconres.2013.11.002.

Yun, H. D., Yang, I. S., Kim, S. W., Jeom, E., Choi, C. S., and Fukuyama, H. (2007). "Mechanical properties of High-Performance Hybrid-Fibre Reinforced Cementitious Composites (HPHFRCCS)." *Magazine of Concrete Research*, Vol. 59, No. 4, pp. 257-271, DOI: 10.1680/macr.2007.59.4.257.

Zhou, X., Ghaffar, S. H., Dong, W., Oladiran, O., and Fan, M. (2013). "Fracture and impact properties of short discrete jute fibre-reinforced cementitious composites." *Materials and Design*, Vol. 49, pp. 35-47, DOI: 10.1016/j.matdes.2013.01.029.